Fast Ca^{2+}-dependent inactivation of the store-operated Ca^{2+} current (I_{SOC}) in liver cells: a role for calmodulin

Tom Litjens[1], M. Lyn Harland[2], Michael L. Roberts[1], Gregory J. Barritt[2] and Grigori Y. Rychkov[1]

[1] *School of Molecular and Biomedical Science, University of Adelaide, Adelaide, South Australia 5005, Australia*
[2] *Department of Medical Biochemistry, School of Medicine, Flinders University of South Australia, Adelaide, South Australia 5001, Australia*

Store-operated Ca^{2+} channels (SOCs) provide a major pathway for Ca^{2+} entry in non-excitable cells. SOCs in immortalized liver cells are highly selective for Ca^{2+} over other cations and are similar to well-studied Ca^{2+} release activated Ca^{2+} (CRAC) channels in haematopoietic cell lines. In the present work, employing H4IIE liver cells, we investigated fast inactivation of SOC current (I_{SOC}), which occurs at membrane potentials below −60 mV. This inactivation was significantly reduced when BAPTA, a faster Ca^{2+} buffer, was used instead of EGTA, and was completely abolished if Na^+ was used as a charge carrier in the absence of divalent cations in the external medium. These results suggested that fast inactivation of SOCs in H4IIE cells was Ca^{2+} dependent and was similar to the fast inactivation of CRAC channels. Experiments showing that the fast inactivation of I_{SOC} was not affected by the disruption of actin by latrunculin B indicate that the cytoskeleton is unlikely to be involved. To elucidate the mechanism of Ca^{2+} dependence, a possible role of calmodulin (CaM) in SOCs' fast inactivation was investigated. The CaM inhibitors Mas-7 and calmidazolium failed to affect I_{SOC} fast inactivation, whereas over-expression of a CaM inhibitor peptide or a mutant CaM lacking functional EF hands significantly altered the inactivation of I_{SOC}. Out of two exponential components normally required to approximate kinetics of I_{SOC} fast inactivation, the faster component was reduced in amplitude by 30%, compared to the control. The results presented suggest that CaM is responsible for at least part of Ca^{2+}-dependent fast inactivation of I_{SOC} in liver cells. It is hypothesized that CaM is tethered to the channel itself and therefore protected from chemical inhibitors.

(Resubmitted 5 April 2004; accepted after revision 28 April 2004; first published online 30 April 2004)
Corresponding author G. Rychkov: School of Molecular and Biomedical Science, University of Adelaide, Adelaide, South Australia, 5005, Australia. Email: grigori.rychkov@adelaide.edu.au

Extracellular agents that affect intracellular processes employ a system of second messengers to communicate the specific signal across the plasma membrane to a target inside the cell. Among the known second messengers, cytoplasmic Ca^{2+} is one of the most widely utilized. A wide variety of hormones, neurotransmitters and growth factors use Ca^{2+} as an intracellular signal to initiate cellular responses (Berridge *et al.* 2003). The specificity of these responses is defined by the magnitude, duration, and location of the increase in the cytoplasmic Ca^{2+} concentration as well as by the intracellular distribution of the Ca^{2+} binding target enzymes (Cancela *et al.* 2002). In non-excitable cells such as those of the immune system, endothelium and epithelium, Ca^{2+} influx through store-operated Ca^{2+} channels (SOCs) is thought to play a major role in maintenance of Ca^{2+} oscillations caused by specific agonists, and in cellular Ca^{2+} homeostasis in general (Parekh & Penner, 1997).

There are several types of SOCs in animal cells, distinguished by their cation selectivity, pharmacology and single channel conductance. The Ca^{2+} release-activated Ca^{2+} (CRAC) channel identified in mast cells and lymphocytes has received most study and is the most clearly defined (Hoth & Penner, 1993; Parekh & Penner, 1997). The features that make this channel unique among other SOCs include an extremely low single channel conductance (∼20 fS), a very high selectivity for Ca^{2+}, and fast Ca^{2+}-dependent inactivation at negative potentials (Hoth & Penner, 1993). The latter takes place on a millisecond time scale, and is evident during hyperpolarizing voltage pulses (Zweifach & Lewis, 1995; Fierro & Parekh, 1999). Investigation of the kinetics of the fast inactivation of I_{CRAC} in the presence of two different

 DOI: 10.1113/jphysiol.2004.065870

intracellular Ca^{2+} chelators, EGTA and BAPTA, which bind Ca^{2+} at relatively slow and fast rates, respectively, suggested that the Ca^{2+} binding site that regulates fast inactivation might be located on the CRAC channel itself (Zweifach & Lewis, 1995; Fierro & Parekh, 1999).

SOCs with properties distinctively different from those of the CRAC channel have been identified by patch clamping in other cell types. These include vascular smooth muscle cells, A431 endothelial cells, prostate cancer epithelial cells, and *Drosophila* S2 cells (Trepakova *et al.* 2001; Abeele *et al.* 2003; Li *et al.* 2003; Yeromin *et al.* 2004). Despite significant similarities with I_{CRAC}, store-operated Ca^{2+} currents (I_{SOC}) in all of those cells showed no fast Ca^{2+}-dependent inactivation at negative potentials. Recently we have characterized I_{SOC} in the H4IIE rat liver cell line (Rychkov *et al.* 2001). Properties of I_{SOC} of H4IIE cells examined in that study, such as selectivity for Ca^{2+}, anomalous mole fraction effect in the presence of Ba^{2+}, and block by divalent and trivalent cations, were similar to those of I_{CRAC} in lymphocytes and mast cells (Rychkov *et al.* 2001). The kinetics of I_{SOC} inactivation in liver cells, however, has not been investigated.

In the present work we characterized fast inactivation of I_{SOC} in H4IIE liver cells and investigated possible mechanisms that may underlie this phenomenon. It was found that I_{SOC} inactivates with a double exponential time course during steps to membrane potentials more negative than −60 mV, similar to that of I_{CRAC} in haematopoietic cell lines (Zweifach & Lewis, 1995). Kinetics of I_{SOC} inactivation depended on the nature of the intracellular Ca^{2+} buffer and the permeating cation, suggesting a Ca^{2+}-dependent mechanism. It was shown that the mechanism responsible for fast inactivation is unlikely to be voltage dependent or to involve the actin cytoskeleton. Possible involvement of calmodulin (CaM) in mediating Ca^{2+} dependence of fast inactivation was investigated using CaM inhibitors, and over-expression of the CaM binding domain of type I adenylyl cyclase (amino acids 481–575) or a Ca^{2+}-incompetent mutant of CaM. While CaM inhibitors, such as mastoporan-7 (Mas-7), had no effect on I_{SOC} fast inactivation, over-expression of either CaM binding domain or CaM mutant, significantly altered the fast inactivation of I_{SOC}. The idea that CaM is involved in the Ca^{2+}-dependent gating of liver cell SOCs is consistent with the results.

Methods

Cell culture

H4-IIE cells (ATCC CRL 1548) were cultured at 37°C in 5% (v/v) CO_2 in air in Dulbecco's modified Eagle's medium (DMEM) supplemented with penicillin (100 units ml^{-1}), streptomycin (100 $\mu g\,ml^{-1}$) and 10% (v/v) fetal bovine serum (complete DMEM). The cells were subcultured for a maximum of 15 passages. Cells were cotransfected with cDNA encoding a Ca^{2+}-incompetent mutant CaM (mutant form of CaM lacking four out of four Ca^{2+} binding sites; provided by Dr M. X. Zhu, Ohio State University) (Peterson *et al.* 1999; Zhang *et al.* 2001) or a CaM inhibitor peptide (the CaM binding domain of type I adenylyl cyclase, amino acids 481–575; provided by Professor W. A. Catterall, University of Washington) (Wu *et al.* 1993; Lee *et al.* 1999) plus cDNA encoding an enhanced green fluorescent protein (pEGFP-C1, Clontech). Control cells were transfected with cDNA encoding pEGFP-C1 alone. Cells were transfected using Fugene-6 (Roche Diagnostics Australia, NSW, Australia) according to the manufacturer's protocol and plated onto glass coverslips. After 4 h the cells were washed with DMEM, and incubated at 37°C in antibiotic-free complete DMEM for 48–72 h before patch clamping. Transfected cells were selected on the basis of their expression of EGFP.

Electrophysiology

Whole-cell patch clamping (Hamill *et al.* 1981) was performed at room temperature using a computer-based patch-clamp amplifier (EPC-9, HEKA Elektronik, Lambrecht/Pfalz, Germany) and PULSE software (HEKA Elektronik). The normal bath solution (control solution) contained (mM): NaCl, 140; CsCl, 4; $CaCl_2$, 10; $MgCl_2$, 2; glucose 10; and Hepes, 10; adjusted to pH 7.4 with NaOH. The standard internal solution contained (mM): caesium glutamate, 120; $CaCl_2$ 5; $MgCl_2$ 5; MgATP 1; EGTA, 10; and Hepes, 10; adjusted to pH 7.2 with NaOH. The calculated internal free Ca^{2+} concentration was about 100 nM (EQCAL, Biosoft, Cambridge, UK). In some experiments 10 mM BAPTA was used instead of EGTA to buffer intracellular Ca^{2+}. Depletion of the intracellular Ca^{2+} stores was achieved by addition of both 20 μM InsP_3 (Amersham) and 1 μM thapsigargin (Sigma) to the internal solution. Patch pipettes were pulled from borosilicate glass coated with Sylgard and fire-polished; pipette resistance ranged between 3 and 5 MΩ. Series resistance, for which no compensation was made, did not exceed 25 MΩ. In order to monitor the development of I_{SOC}, voltage ramps between −138 and +102 mV were applied every 2 s, starting immediately after achieving the whole-cell configuration. Acquired currents were filtered at 2.7 kHz and sampled at 10 kHz. All voltages shown have been corrected for the liquid junction potential of −18 mV between the bath and electrode solutions (estimated

by JPCalc; Barry, 1994). The holding potential was −18 mV throughout. Cell capacitance was compensated automatically by the EPC9 amplifier.

Leakage subtraction

First current traces obtained just after breaking into the cell and before I_{SOC} started to develop were used to determine leakage. As I_{SOC} develops in H4IIE cells with little delay, only one or two traces could be used, and there was not enough time to record leakage traces for all voltage protocols used. To ensure that the leakage had not changed during the recording, and to obtain leakage traces at −118, −138 and −158 mV steps, at the end of the experiment 10 μM La^{3+} was applied to the bath to block I_{SOC}. In most cases, the amplitudes of leakage determined before development of I_{SOC} and following the addition of 10 μM of La^{3+} to the bath were the same (± 3%). Exactly the same value was obtained for the leakage current if extracellular Ca^{2+} was replaced with Mg^{2+}, and 100 nM of La^{3+} was added to the bath. The latter method was preferred, as the block by 100 nM La^{3+} was fully reversible when the cells were washed with the solution containing 10 mM Ca^{2+}. The block by 10 μM La^{3+} could not be fully reversed by washing cells with the control solution. In approximately 20% of cells, leakage conductance determined by applying La^{3+} was 20–30% smaller then that measured before I_{SOC} development. This difference was due to the presence of a small outwardly rectifying current that disappeared after 1–2 min of intracellular perfusion. The criterion for the accurate determination of the leakage was the correct shape of the leakage-subtracted *I–V* plots, in particular, the zero current between +60 and +100 mV.

Data analysis

Peak current was measured 2 ms after the beginning of the voltage pulse to minimize possible errors due to residual uncompensated capacitance. Steady state current was determined as the 10 ms average at the end of a 200 ms pulse. To analyse the kinetics of I_{SOC} inactivation, leak-subtracted current traces from different cells obtained under the same conditions were normalized to the peak current and averaged using Prism4 (GraphPad). The resulting traces were fitted by a single or a double exponential function:

$$I(t) = a_1 e^{-t/\tau_1} + c \quad (1a)$$

$$I(t) = a_1 e^{-t/\tau_1} + a_2 e^{-t/\tau_2} + c \quad (1b)$$

where a_1 and a_2 are relative amplitudes of the faster and slower exponential components, respectively, c is the steady state component, and τ_1 and τ_2 are the time constants of the corresponding exponential components. The averaged data are presented as the mean ± S.E.M.

Localization of the actin cytoskeleton

The location of actin filaments was determined using Texas Red–X phalloidin (Bonfoco *et al.* 1996). H4IIE cells grown on collagen-treated coverslips were fixed by 3.5% (v/v) formaldehyde, permeabilized with 0.1% (v/v) Triton X-100, and stained with Texas Red–X phalloidin (Molecular Probes) according to the manufacturer's instructions. Images of the stained cells were obtained by fluorescence microscopy using a Nikon Eclipse TE300 microscope with a Nikon 60 × 1.2 NA Plan Apo objective. A mercury vapour lamp was used as a light source with an excitation filter 510–560 nm and an emission 590 nm long pass filter. Images were captured by a Nikon DXM 1200 camera.

Results

Dependence of I_{SOC} fast inactivation in H4IIE cells on intracellular Ca^{2+} buffer

In H4IIE liver cells under control conditions (10 mM EGTA in the pipette with 100 nM free Ca^{2+}, and 10 mM $CaCl_2$ in the bath solution), I_{SOC} recorded in response to 200 ms voltage steps to potentials ranging from −118 to −158 mV showed marked inactivation (Fig. 1*A*). Raising the concentration of free Ca^{2+} in the pipette solution up to ∼500 nM while reducing the concentration of EGTA to 1 mM had no effect on the kinetics of fast inactivation of I_{SOC} (not shown). Using BAPTA as the intracellular Ca^{2+} buffer in the pipette solution in place of EGTA, however, resulted in a significant reduction of I_{SOC} inactivation (Fig. 1*B*). The relative amplitude of the steady state current measured at the end of 200 ms pulse to −158 mV increased from ∼0.32 in the control conditions to ∼0.60 in the presence of BAPTA (Table 1). At membrane potentials more negative than −118 mV the inactivating component of I_{SOC} could be reliably fitted by the sum of two exponentials (eqn (1b)), while a single exponential fit (eqn (1a)) was clearly not sufficient (Fig. 1*C*). With BAPTA in the pipette solution, currents recorded in response to hyperpolarizing steps to −118 mV inactivated with a single exponential time course. At more negative potentials, however, a double exponential fit was somewhat better than a single exponential fit

($P < 0.001$, compared using an F test in Prism4; Fig. 1*C*). The main difference between currents recorded with BAPTA and those with EGTA was a smaller amplitude of the faster exponential component (a_1) and a larger steady state component (c), while the amplitude of the slower exponential component (a_2) remained unchanged, as well as the time constants of both exponential components (eqn (1b); Table 2). Despite a significant difference in the rate of fast inactivation between currents recorded with EGTA and BAPTA as the intracellular Ca^{2+} buffers, there was little difference between the *I–V* plots of I_{SOC} under the two conditions (Fig. 1*D*), suggesting that the faster exponential component (a_1) of inactivation plays a minor role in determining the shape of *I–V* plots obtained in response to 100 ms ramps.

Dependence of I_{SOC} fast inactivation on charge carrier

Dependence of I_{SOC} fast inactivation on the intracellular Ca^{2+} buffer suggested Ca^{2+} involvement in its regulation. To further investigate dependence of fast inactivation on Ca^{2+}, in the next series of experiments Ba^{2+} or Sr^{2+} was used instead of Ca^{2+} as charge carrier. When recorded with Ba^{2+} or Sr^{2+}, I_{SOC} still showed significant inactivation (Fig. 2*A* and *B*); its kinetics, however, were different from that observed with Ca^{2+} as the charge carrier (Table 2). At −118 mV, currents with both Ba^{2+} and Sr^{2+}, but not with Ca^{2+}, could be fitted with a single exponential function (Fig. 2*D*, Table 2). At more negative potentials (−158 mV), however, there was no qualitative difference as all currents with Ba^{2+}, Sr^{2+}, or Ca^{2+} required a double exponential fit

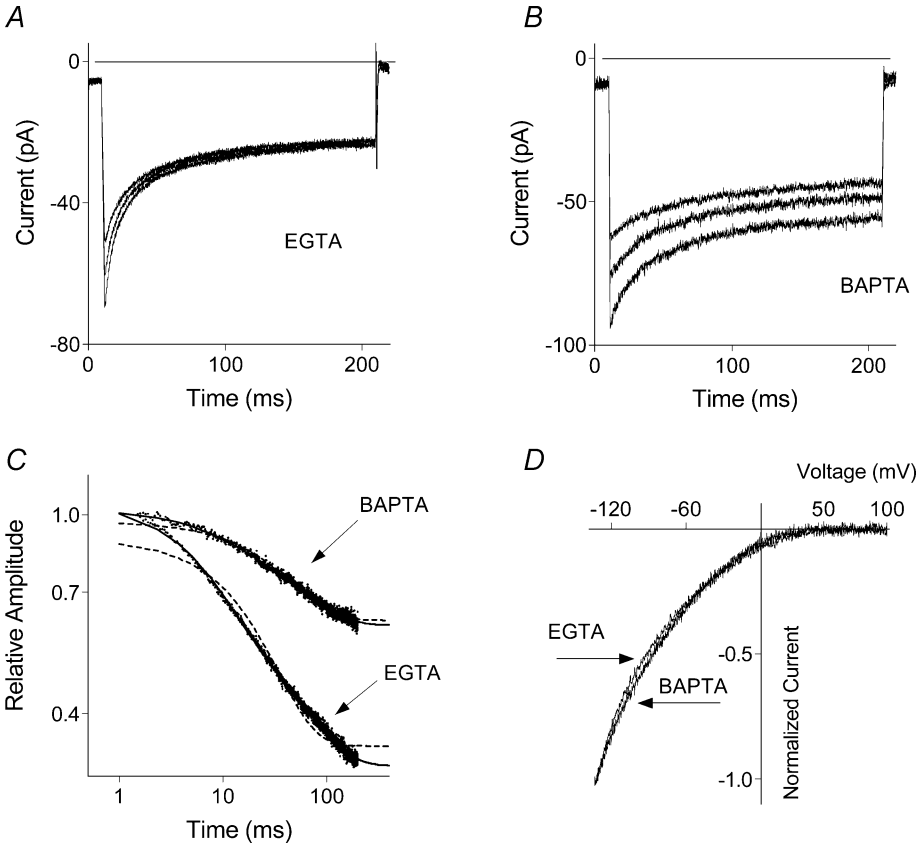

Figure 1. Dependence of the fast inactivation of I_{SOC} on the nature of the intracellular Ca^{2+} buffer
I_{SOC} was recorded in response to 200 ms steps to −118, −138 and −158 mV in the control conditions with 10 mM EGTA in the pipette (~100 nM free Ca^{2+}) (*A*), and with 10 mM BAPTA (~100 nM free Ca^{2+}) instead of EGTA in the pipette solution (*B*). *C*, kinetics of I_{SOC} fast inactivation. I_{SOC} recorded in response to 200 ms steps to −158 mV is shown on a log–log scale for the control conditions and with BAPTA as intracellular buffer. Currents were normalized to a maximal peak current. Dashed lines represent a single exponential fit (eqn (1a)), and the continuous lines a double exponential fit (eqn (1b)). Each trace on this and other graphs, unless specified otherwise, is an average of a number of traces obtained from different cells (for *n* see Table 1). *D*, *I–V* plots of I_{SOC} obtained in response to 100 ms voltage ramps from −138 mV to 102 mV under control condition (EGTA) and in the presence of BAPTA. Currents were normalized to the maximal amplitude at −138 mV.

Table 1. The effect of different experimental conditions tested on the steady state component of I_{CRAC}

Voltage	Control ($n = 15$)	BAPTA ($n = 4$)	Sr^{2+} ($n = 9$)	CaM mutant ($n = 12$)	CaM peptide ($n = 14$)	Latrunculin ($n = 10$)
−118 mV	0.44 ± 0.019	0.69 ± 0.041***	0.51 ± 0.019**	0.50 ± 0.023*	0.55 + 0.021**	0.48 ± 0.027
−138 mV	0.37 ± 0.018	0.65 ± 0.035***	0.47 ± 0.020**	0.45 ± 0.020*	0.49 ± 0.023**	0.41 ± 0.024
−158 mV	0.32 ± 0.017	0.60 ± 0.032***	0.46 ± 0.021**	0.44 ± 0.025**	0.49 ± 0.023***	0.36 ± 0.023

Values are the relative amplitude of the steady state component of I_{CRAC}. The steady state component was measured as a 10 ms average at the end of the 200 ms pulse (see Methods). The values are shown as the mean ± S.E.M. of the number experiments identified in brackets. Degrees of significance, determined by *t* test, are $^{*}P < 0.05$, $^{**}P < 0.01$, $^{***}P < 0.001$.

Table 2. The effect of different experimental conditions on the kinetic parameters of I_{SOC} inactivation

Voltage	Parameter	Control ($n = 15$)	BAPTA ($n = 4$)	Sr^{2+} ($n = 9$)	Ba^{2+} ($n = 7$)	CaM mutant ($n = 14$)	CaM peptide ($n = 10$)
−118 mV	a_1	0.25 ± 0.018	n.d.	n.d.	n.d.	0.19 ± 0.021*	0.18 ± 0.025*
	a_2	0.32 ± 0.019	0.31 ± 0.027	0.48 ± 0.021	0.46 ± 0.016	0.31 ± 0.023	0.28 ± 0.023
	c	0.43 ± 0.016	0.69 ± 0.030	0.52 ± 0.020	0.54 ± 0.015	0.50 ± 0.020*	0.54 ± 0.021***
	τ_1 (ms)	9.6 ± 0.9	n.d.	n.d.	n.d.	10.7 ± 1.2	11.5 ± 1.0
	τ_2 (ms)	58 ± 5	59 ± 9	50 ± 8	60 ± 8	62 ± 7	67 ± 7
−138 mV	a_1	0.35 ± 0.020	n.d.	0.15 ± 0.025***	0.20 ± 0.021***	0.24 ± 0.019**	0.26 ± 0.021**
	a_2	0.29 ± 0.017	0.34 ± 0.025	0.38 ± 0.023**	0.37 ± 0.021*	0.31 ± 0.023	0.26 ± 0.020
	c	0.36 ± 0.019	0.66 ± 0.029	0.47 ± 0.020**	0.43 ± 0.020*	0.45 ± 0.018**	0.48 ± 0.023***
	τ_1 (ms)	9.5 ± 1.0	n.d.	11.0 ± 1.3	14.0 ± 2.0*	7.9 ± 1.0	10.0 ± 1.2
	τ_2 (ms)	62 ± 6	53 ± 9	47 ± 6	70 ± 9	51 ± 6	63 ± 8
−158 mV	a_1	0.41 ± 0.017	0.12 ± 0.030***	0.24 ± 0.021***	0.28 ± 0.021***	0.26 ± 0.019***	0.29 ± 0.023***
	a_2	0.28 ± 0.016	0.28 ± 0.030	0.30 ± 0.023	0.33 ± 0.020	0.30 ± 0.020	0.22 ± 0.020
	c	0.31 ± 0.016	0.60 ± 0.029***	0.46 ± 0.024***	0.38 ± 0.020*	0.44 ± 0.019***	0.49 ± 0.020***
	τ_1 (ms)	8.1 ± 0.8	9.9 ± 1.2	8.3 ± 0.6	10 ± 1.1	6.9 ± 0.9	8.8 ± 1.0
	τ_2 (ms)	59 ± 4	59 ± 9	41 ± 5	54 ± 6	42 ± 7	54 ± 5

The values are shown as the mean ± S.E.M. of the number experiments identified in brackets. a_1 and a_2 represent the relative amplitudes of the fast and slow exponential components, respectively, τ_1 and τ_2 are the time constants (ms) of these components, and c is the relative amplitude of the steady state component (eqn (1b)); n.d. – not detectable. Degrees of significance, determined by *t* test, are $^{*}P < 0.05$, $^{**}P < 0.01$, $^{***}P < 0.001$.

(Fig. 2*E* and *F*); while quantitatively, I_{SOC} inactivated less with Ba^{2+} and Sr^{2+}. Thus the steady state current at the end of a 200 ms pulse increased to ∼0.40 and 0.46 with Ba^{2+} and Sr^{2+}, respectively, compared to ∼0.32 with Ca^{2+} (Table 1). Increase of the steady state component of the current occurred as a result of the decrease of the amplitude of the faster exponential component (Table 2). As reported previously for I_{CRAC} in haematopoietic cell lines (Hoth, 1995), I_{SOC} recorded in H4IIE cells with either Ba^{2+} or Sr^{2+} showed a complex dependence on divalent cation concentration and time (results not shown). *I–V* plots recorded with Ba^{2+} or Sr^{2+} as charge carriers showed much stronger inward rectification than that observed with Ca^{2+}, with relative slope conductance at potentials negative to −100 mV following the sequence $Ba^{2+} > Sr^{2+} > Ca^{2+}$ (Fig. 2*C*).

Ba^{2+} and Sr^{2+} did not remove most of the fast inactivation of I_{SOC} in liver cells, which could be explained in two ways: (i) these divalent cations can replace Ca^{2+} to a certain extent at the Ca^{2+} binding site that regulates fast inactivation; or (ii) a significant part of fast inactivation is Ca^{2+} independent. To investigate the latter possibility currents were recorded in divalent-free external solution (Fig. 3). After full development of I_{SOC}, the control solution was replaced with divalent free solution supplemented with 2 mM EDTA, which resulted in a sharp increase (4- to 6-fold; $n = 9$) and subsequent decline of the current amplitude (Fig. 3*A*). *I–V* plots recorded in the divalent-free solution showed strong inward rectification and a reversal potential of about +30 mV, suggesting higher permeability for Na^{+} compared to Cs^{+} (Fig. 3*B*). Currents recorded in response to 200 ms voltage steps to

potentials between −158 and −118 mV showed no fast inactivation (Fig. 3*C*).

Effect of disruption of the cytoskeleton

It has been shown that Ca^{2+}-dependent inactivation of some Ca^{2+} channels may depend on the integrity of the cytoskeleton (Gera & Byerly, 1999). We investigated dependence of I_{SOC} inactivation on the integrity of the cytoskeleton by using a marine toxin, latrunculin B (Calbiochem), which disrupts microfilament organization 10–100 times more potently than cytochalasins (Spector *et al.* 1989). After incubation of the cells for 60 min at 37°C with 10 μM latrunculin there were significant changes in cell morphology: most of the cells were spherical in shape, which was evidently a result of the cytoskeleton disruption. Only those cells that were visibly affected by latrunculin, were selected for patch clamping. Staining by Texas Red–X phalloidin revealed that actin in cells treated with latrunculin B was less organized compared to that in untreated cells (Fig. 4). Nevertheless, I_{SOC} developed in these treated cells at the same rate as that in untreated cells, and no change in the maximal amplitude of the current was observed (Fig. 5*A*). There was no significant change in the kinetics of fast inactivation in cells treated with latrunculin B, compared to the control cells (Fig. 5*B*). A small increase of the steady state current after treatment with latrunculin was below statistical significance (Fig. 5*B* and Table 1).

Effect of calmodulin inhibitors on I_{SOC}

We have previously reported that CaM inhibitors like calmidazolium (Sigma, 20 μM in the external solution) and CaM-dependent protein kinase II peptide 290–309 (Sigma, 1–10 μM in the pipette) had no effect on the

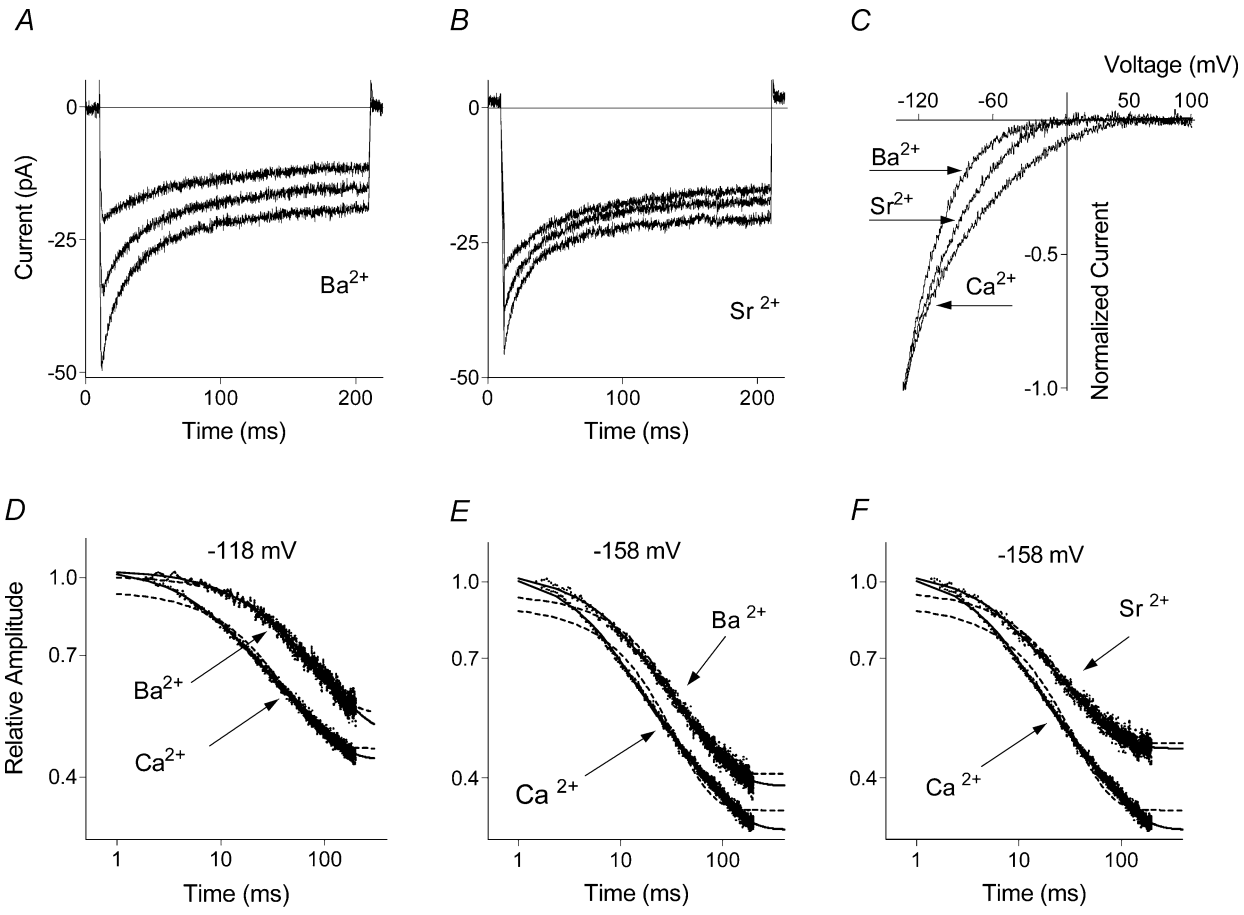

Figure 2. Dependence of the fast inactivation of I_{SOC} on the charge carrier
I_{SOC} recorded with Ba^{2+} (*A*) and Sr^{2+} (*B*) as the charge carriers. *C*, *I–V* plots of I_{SOC} obtained with Ca^{2+}, Ba^{2+} and Sr^{2+}. *D*, *E* and *F*, kinetics of I_{SOC} fast inactivation with Ba^{2+} (*D* and *E*) and Sr^{2+} (*F*) as the charge carriers. Normalized values of I_{SOC} are shown on a log–log scale. Dotted lines represent a single exponential fit (eqn (1a)) and the solid lines are a double exponential fit (eqn (1b)). Parameters of the fits are presented in Table 2.

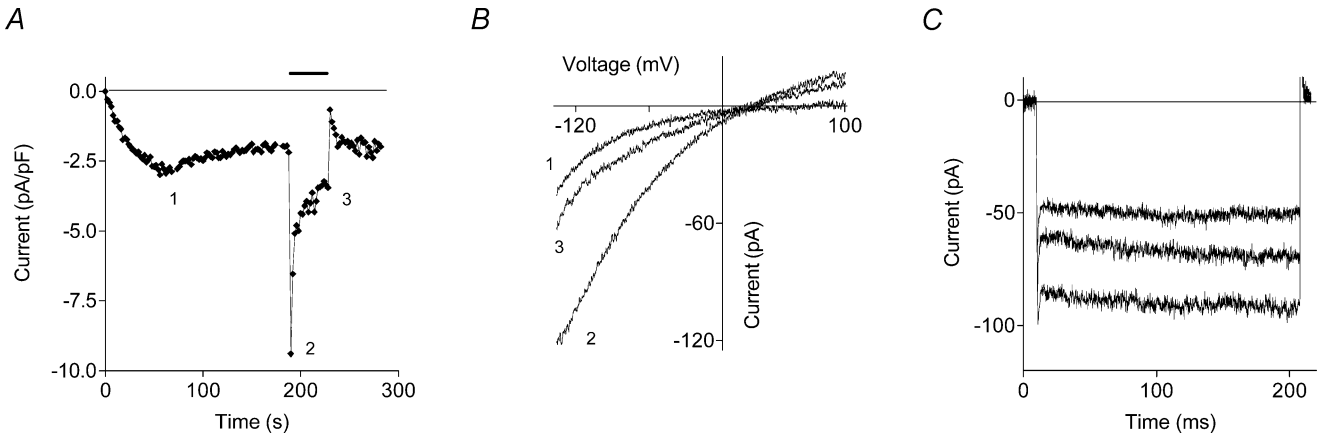

Figure 3. Monovalent currents through SOCs in divalent-free external solution
A, effect of replacement of control solution with divalent-free solution on the amplitude of I_{SOC}. Amplitude at −118 mV is plotted against time. Horizontal bar shows time of the application of divalent-free solution. *B*, *I–V* plots of I_{SOC} obtained in control conditions (trace 1) and divalent-free solution (traces 2 and 3). *C*, current traces obtained in divalent-free solution in response to voltage steps to −118, −138, and −158 mV steps. Results shown on this figure are from a cell representative of 8 cells with similar results.

development or the amplitude of I_{SOC} in H4IIE cells (Rychkov *et al.* 2001). Moreover, they did not significantly affect the fast inactivation of I_{SOC} (results not shown). Another cell-permeant CaM inhibitor investigated in the present study, Mas-7 (Calbiochem), also failed to alter either I_{SOC} development or the kinetics of its inactivation at negative potentials (Fig. 6).

Effects of expression of a dominant negative CaM mutant and a CaM inhibitor peptide

Lack of the effect of the CaM inhibitors such as calmidazolium has previously been reported for L-type Ca^{2+} channels and Ca^{2+}-activated SK channels (Xia *et al.* 1998; Zuhlke & Reuter, 1998). In subsequent experiments,

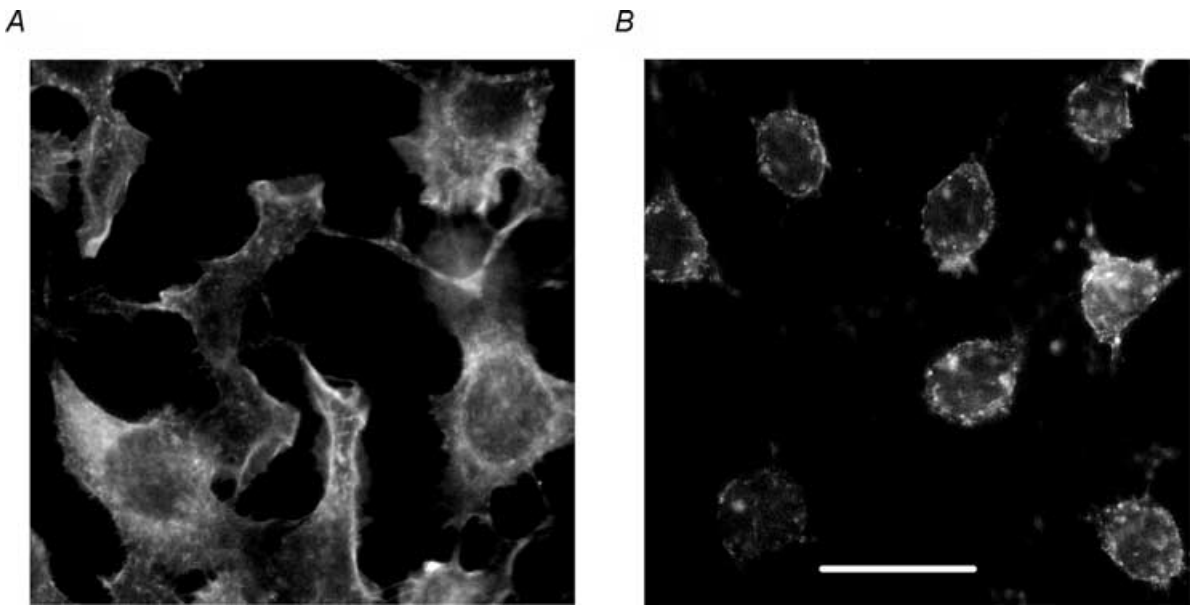

Figure 4. Disruption of cytoskeleton in H4IIE cells by latrunculin B
Cells were incubated for 30 min either in the absence (*A*) or presence of 10 μM latrunculin B (*B*) before fixation and staining of actin with Texas Red–X phalloidin. Horizontal bar represents 20 μm.

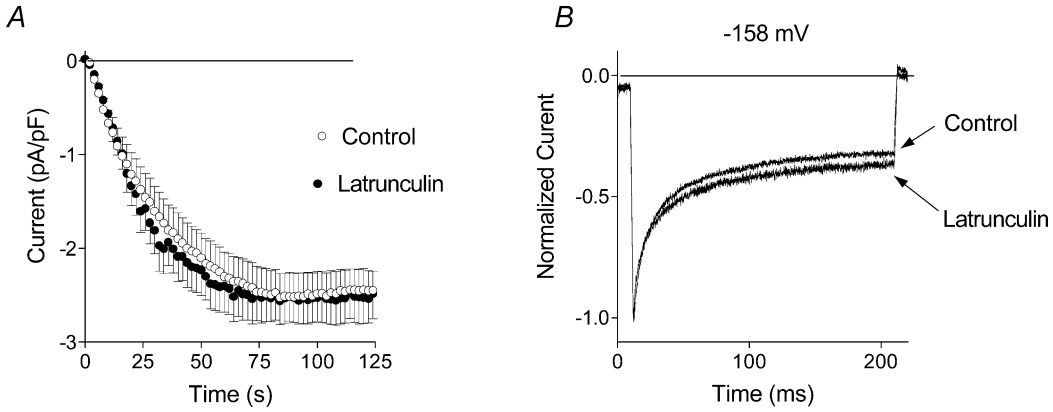

Figure 5. Effect of latrunculin B on I_{SOC}
A, development of I_{SOC} in control cells and in cells treated with 10 μM latrunculin B. Each point represents the amplitude of I_{SOC} at −118 mV taken from voltage ramps from −138 to 102 mV, applied every 2 s. *B*, normalized and averaged current traces in response to −158 mV steps in control conditions ($n = 15$) and after treatment with latrunculin B ($n = 10$).

however, it was shown that these channels are regulated by CaM that is permanently tethered to the channel protein and is not accessible to these inhibitors (Zuhlke *et al.* 1999). Over-expression of a CaM dominant negative mutant or a CaM inhibitor peptide in H4IIE cells had little effect on the time course of I_{SOC} development. The time constants of activation were 32 ± 6 s ($n = 9$) in control cells, and 43 ± 8 s ($n = 8$) and 39 ± 7 s ($n = 8$) in cells expressing the CaM mutant or the CaM inhibitor peptide, respectively, and were not statistically different (Fig. 7*A*). The amplitude of I_{SOC} measured at −100 mV from *I–V* plots recorded in response to voltage ramps also remained unchanged at about -2.5 pA pF^{-1} in cells expressing the CaM mutant or the CaM inhibitor peptide. The shape of the *I–V* plot for I_{SOC} did not change in cells transfected with the CaM mutant or the CaM inhibitor peptide (Fig. 7*B*). This confirms that over-expression of mutant CaM or CaM inhibitor peptide did not introduce any additional current in H4IIE cells, and that the leakage in the transfected cells was determined with the same accuracy as that in non-transfected cells.

In cells expressing the CaM mutant or the CaM inhibitor peptide there was a noticeable change in the kinetics of current inactivation at membrane potentials more negative than −80 mV (Figs 7*C* and 8, and Table 1). The amplitude of the steady state current at the end of the 200 ms pulse significantly increased in comparison with that in control cells. Currents in transfected cells could be fitted with the same equation (eqn (1b)) as the I_{SOC} in control cells (Fig. 9 and Table 2). Compared with the control, there was a significant reduction of the relative amplitude of the faster exponential component (a_1) and an

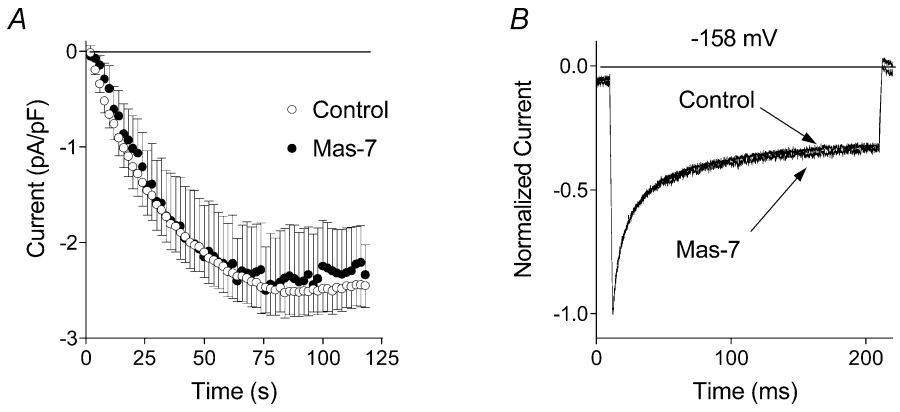

Figure 6. Effect of Mas-7 on I_{SOC}
A, development of I_{SOC} in control cells and in cells treated with 10 μM Mas-7. Each point represents the amplitude of I_{SOC} at −118 mV taken from voltage ramps from −138 to 102 mV applied every 2 s. *B*, normalized and averaged current traces in response to −158 mV steps in control conditions ($n = 15$) and after treatment with Mas-7 ($n = 9$).

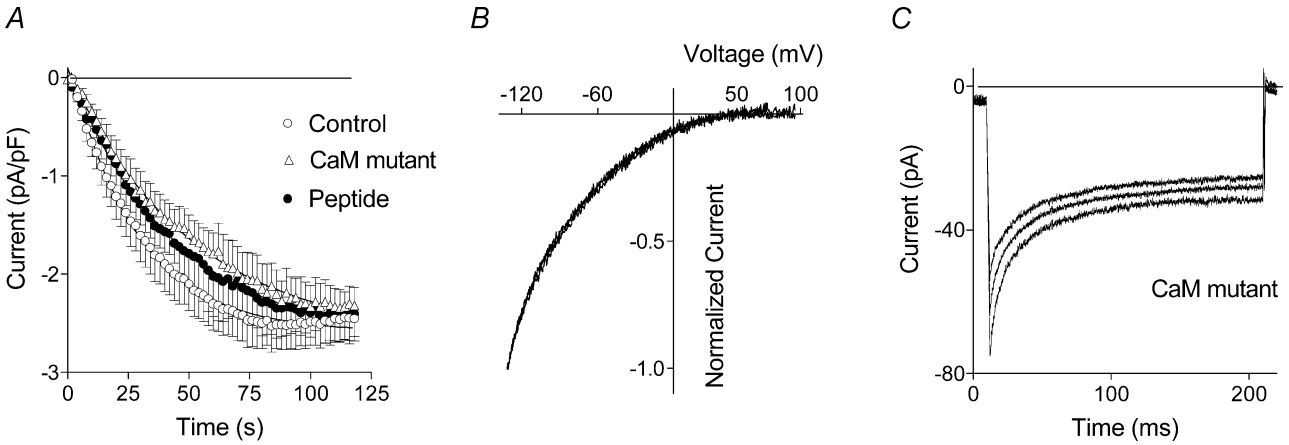

Figure 7. I_{SOC} in cells expressing a dominant negative mutant CaM and a CaM inhibitor peptide
A, development of I_{SOC} in control cells and in cells expressing a dominant negative mutant CaM and a CaM inhibitor peptide. *B*, normalized *I–V* plots of I_{SOC} in control cells and in cells expressing a dominant negative mutant CaM. (The *I–V* plot for I_{SOC} from cells expressing a CaM inhibitor peptide is completely superimposed on the other two *I–V* plots and is not shown for clarity.) *C*, I_{SOC} in response to 200 ms steps to −118, −138 and −158 mV recorded in the cells expressing dominant negative mutant CaM ($n = 12–15$).

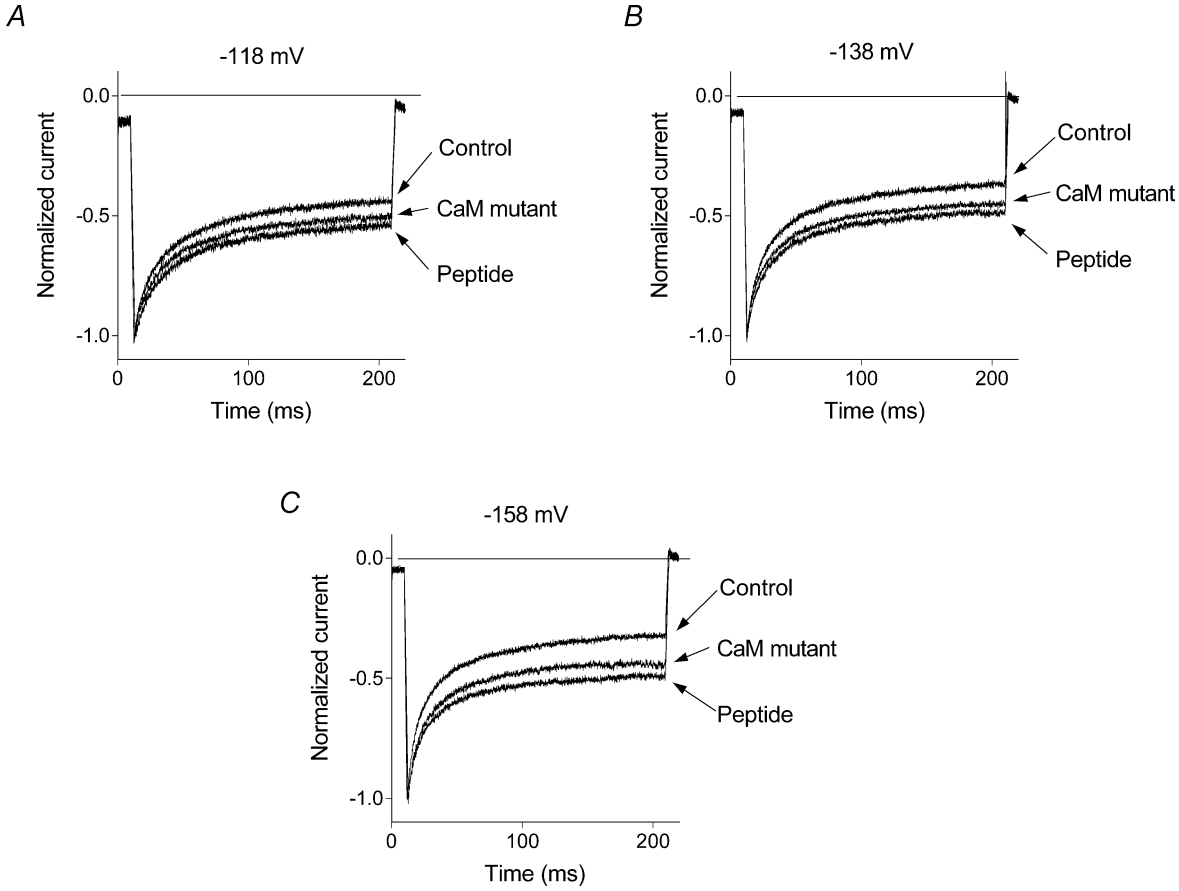

Figure 8. Effect of CaM suppression on the fast inactivation of I_{SOC}
Normalized averaged traces of I_{SOC} recorded in response to −118 mV (*A*), −138 mV (*B*), and −158 mV (*C*) in control cells and cells expressing a dominant negative mutant CaM and a CaM inhibitor peptide ($n = 12–15$).

increase in the amplitude of the steady state component (c), while the time constants of both exponential components did not change (Table 2). The amplitude of the faster exponential component was reduced by 25–35% in cells expressing either the CaM mutant or the CaM inhibitor peptide compared to the control cells. The relative reduction of the fast exponential component was the same (compared using a t test) at all membrane potentials tested.

Transfection of H4IIE cells with cDNA encoding wild-type CaM had no effect on either I_{SOC} development, or kinetics of fast inactivation ($n = 6$; results not shown)

Discussion

The experiments in this work were designed to characterize fast inactivation of I_{SOC} in H4IIE liver cells and to investigate the underlying mechanism. It has been found that, at membrane potentials below −100 mV, fast inactivation of I_{SOC} follows a double exponential time course with the time constants of about 7–15 ms (τ_1) for the faster component (a_1) and 50–100 ms (τ_2) for the slower component (a_2). The extent of fast inactivation strongly depended on the nature of the intracellular Ca^{2+} buffer, being less prominent with the faster Ca^{2+} chelator BAPTA. Replacement of EGTA with BAPTA only affected the faster exponential component of inactivation. This component could not be reliably detected at voltage steps to −118 mV and −138 mV and was reduced by 70% at −158 mV steps. Dependence on the nature of the Ca^{2+} buffer suggested a Ca^{2+}-dependent mechanism for at least one component of inactivation. This was further investigated by replacing Ca^{2+} with Ba^{2+} and Sr^{2+}. Both divalent cations changed the kinetics of fast inactivation, again mainly affecting the amplitude of the faster exponential component; however, some effect on the slower component was evident at −138 mV steps.

Although the effects of Ba^{2+} and Sr^{2+} on I_{SOC} kinetics were significant, they were far less drastic than that reported for L-type voltage-dependent Ca^{2+} channels, where Ba^{2+} or Sr^{2+} removed most of the fast inactivation, which was predominantly Ca^{2+} dependent (Zuhlke *et al.* 1999). This may imply that the site that regulates Ca^{2+}-dependent inactivation in voltage-dependent Ca^{2+} channels is more selective for Ca^{2+} than the corresponding site in the liver cell SOC. An alternative explanation, that a significant part of the fast inactivation of I_{SOC} is not Ca^{2+} dependent, is unlikely, as Na^+ currents through SOCs recorded in H4IIE cells had no fast inactivation present at voltage steps to all membrane potentials, which supports the notion that all of the fast inactivation of I_{SOC} seen in the presence of Ca^{2+} is Ca^{2+} dependent. These results also suggest that two exponential components of I_{SOC} fast inactivation may reflect Ca^{2+} binding to two different Ca^{2+} binding sites. One of these sites is apparently unaffected by BAPTA, while both of those sites can bind Ba^{2+} and Sr^{2+}, although, compared with Ca^{2+}, with a diminished capacity. The exact nature of two components of fast inactivation, however, remains unresolved.

I_{SOC} in H4IIE cells has many features similar to those of I_{CRAC} in haemopoietic cell lines, particularly, high selectivity for Ca^{2+} over Na^+, and block by a range of divalent and trivalent cations (Hoth & Penner, 1993; Rychkov *et al.* 2001). Single channel currents in

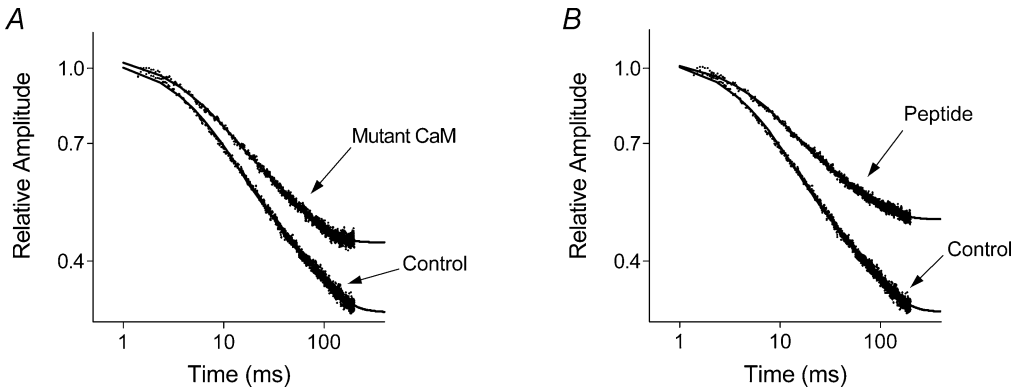

Figure 9. Kinetics of I_{SOC} fast inactivation in cells expressing dominant negative mutant CaM and CaM inhibitor peptide

I_{SOC} recorded in response to 200 ms steps to −158 mV is shown on a log–log scale for the cells expressing mutant CaM (*A*), and CaM inhibitor peptide (*B*). Averaged currents from 12–15 cells in each condition were normalized to a maximal peak current. Continuous lines are a double exponential fit of eqn (1b) to the experimental points. Parameters of the fits are shown in Table 2.

divalent-free external solution that have been previously attributed to the SOCs in H4IIE cells are likely to be a result of the activity of another channel regulated by intracellular Mg^{2+} (Prakriya & Lewis, 2002). In the present study we used 5 mM $MgCl_2$ in the pipette solution to suppress the activity of those channels. As a result, no single-channel events were detectable in divalent-free medium, and monovalent currents in H4IIE cells showed characteristics similar to that of I_{CRAC} carried by Na^+, i.e. strong inward rectification, and selectivity for Na^+ over Cs^+ (Hermosura *et al.* 2002). Fast inactivation of I_{SOC}, particularly the presence of two exponential components, dependence on BAPTA, and absence of fast inactivation in divalent-free external solution were also similar to those of I_{CRAC} (Prakriya & Lewis, 2003; present study). There were some differences, however, regarding currents carried by Ba^{2+}. In Jurkat T-lymphocytes Ba^{2+} current seemed to inactivate less than that observed for Ba^{2+} in the present study (Zweifach & Lewis, 1995), while in RBL-1 cells Ba^{2+} currents were too small for analysis (Fierro & Parekh, 1999), which was not the case in H4IIE cells. Dependence of the fast inactivation on the Ca^{2+} binding kinetics of the buffer employed and independence of the bulk cytoplasmic Ca^{2+} concentration implies that the Ca^{2+} binding site that regulates fast inactivation is located very close to the internal mouth of the channel. In fact, calculations by Zweifach & Lewis (1995) predict that the Ca^{2+} binding site is situated 3–4 nm from the mouth of the CRAC channel and may be a part of the channel itself.

A common mechanism that mediates the Ca^{2+} dependence of ion channels involves CaM, a small soluble protein which can bind up to four Ca^{2+} and cause conformational changes in the target protein (Saimi & Kung, 2002). CaM is known to regulate the function of ion channels both through a direct interaction with the channel and through CaM-dependent enzymes (for review see Saimi & Kung, 2002). As fast inactivation depends only on the local Ca^{2+} concentration in the channel mouth (Zweifach & Lewis, 1995), regulation by a Ca^{2+}-dependent enzyme located in the cytoplasmic space some distance from the SOC is unlikely. Therefore, if CaM is involved in fast inactivation, it is unlikely to be freely mobile in the cytoplasmic space. This conclusion is consistent with the results of the present study, which indicate that fast inactivation of I_{SOC} was unaffected by the CaM inhibitors Mas-7 and calmidazolium. A possibility that CaM or another Ca^{2+}-dependent enzyme is anchored by the actin skeleton close to the internal mouth of the channel is also unlikely, as the present results showed that disruption of the actin cytoskeleton had little effect on I_{SOC} fast inactivation. This also showed that the fast inactivation mechanism of the SOC in H4IIE cells does not directly depend on integrity of the actin cytoskeleton, in contrast to some voltage-dependent Ca^{2+} channels (Gera & Byerly, 1999; Sadeghi *et al.* 2002).

Ca^{2+}-dependent inactivation of L- and P/Q-type voltage-dependent Ca^{2+} channels is mediated by CaM but is not affected by CaM inhibitors such as calmidazolium (Zuhlke *et al.* 1999). This is because CaM in those channels is constitutively tethered to the channel protein and therefore protected from inhibitors dissolved in the cytoplasm (Lee *et al.* 2000; DeMaria *et al.* 2001). The involvement of CaM in the gating of these Ca^{2+} channels has been shown by expressing a Ca^{2+}-incompetent CaM mutant or a CaM inhibitor peptide with the channel of interest (Lee *et al.* 1999, 2000; DeMaria *et al.* 2001). A CaM inhibitor peptide would decrease the free CaM concentration in the cytoplasmic space and therefore would decrease both Ca^{2+}-dependent binding and Ca^{2+}-independent tethering of CaM to the target proteins. In contrast, a Ca^{2+}-incompetent CaM mutant would have no effect on the Ca^{2+}-dependent CaM binding to its targets, because it lacks Ca^{2+} binding sites, but would compete with the wild-type CaM for the tethering sites, and therefore have a dominant negative effect only on the processes that are regulated by tethered CaM.

Expression of either a CaM inhibitor peptide or a Ca^{2+}-incompetent CaM mutant in H4IIE cells resulted in a diminished fast inactivation of I_{SOC} seen as an increased steady state current at the end of a 200 ms pulse. Analysis of the current kinetics revealed that only the amplitude of the faster exponential component was affected, which was reduced by about 30%. The same component was also reduced by intracellular BAPTA, although to a much greater extent. The conclusion that can be made from these results is that CaM does participate in SOC gating, being responsible for at least 30% of the faster component of inactivation. It is impossible to say, however, if it constitutes the whole mechanism. There could be two reasons for incomplete removal of the faster component of inactivation by CaM mutant. Firstly, not all endogenous CaM might have been replaced by mutant CaM in the 48–72 h post-transfection, so the cells most likely contained mixtures of putative SOCs associated with wild-type and mutant CaM. Secondly, Ca^{2+}-dependent fast inactivation of I_{SOC} may be partly mediated by CaM and partly by Ca^{2+} binding to the channel itself. The possibility that Ca^{2+} binds directly to the SOC cannot be dismissed, as the molecular identity of the channel is not known, and the presence or absence of Ca^{2+} binding sites and/or CaM binding sites is yet to be established. The fact that Ca^{2+}-incompetent CaM mutant does have an effect on

fast inactivation, while CaM inhibitors do not, suggests that CaM is permanently tethered to SOC in H4IIE cells; however, the final proof of that has to wait for this channel to be cloned.

References

Abeele FV, Shuba Y, Roudbaraki M, Lemonnier L, Vanoverberghe K, Mariot P, Skryma R & Prevarskaya N (2003). Store-operated Ca^{2+} channels in prostate cancer epithelial cells: function, regulation, and role in carcinogenesis. *Cell Calcium* **33**, 357–373.

Barry PH (1994). JPCalc, a software package for calculating liquid junction potential corrections in patch-clamp, intracellular, epithelial and bilayer measurements and for correcting junction potential measurements. *J Neurosci Meth* **51**, 107–116.

Berridge MJ, Bootman MD & Roderick HL (2003). Calcium signalling: dynamics, homeostasis and remodelling. *Nat Rev Mol Cell Biol* **4**, 517–529.

Bonfoco E, Leist M, Zhivotovsky B, Orrenius S, Lipton SA & Nicotera P (1996). Cytoskeletal breakdown and apoptosis elicited by NO donors in cerebellar granule cells require NMDA receptor activation. *J Neurochem* **67**, 2484–2493.

Cancela JM, Van Coppenolle F, Galione A, Tepikin AV & Petersen OH (2002). Transformation of local Ca^{2+} spikes to global Ca^{2+} transients: the combinatorial roles of multiple Ca^{2+} releasing messengers. *EMBO J* **21**, 909–919.

DeMaria CD, Soong TW, Alseikhan BA, Alvania RS & Yue DT (2001). Calmodulin bifurcates the local Ca^{2+} signal that modulates P/Q-type Ca^{2+} channels. *Nature* **411**, 484–489.

Fierro L & Parekh AB (1999). Fast calcium-dependent inactivation of calcium release-activated calcium current (CRAC) in RBL-1 cells. *J Membr Biol* **168**, 9–17.

Gera S & Byerly L (1999). Voltage- and calcium-dependent inactivation of calcium channels in *Lymnaea* neurons. *J General Physiol* **114**, 535–550.

Hamill OP, Marty A, Neher E, Sakmann B & Sigworth FJ (1981). Improved patch-clamp techniques for high-resolution current recording from cells and cell-free membrane patches. *Pflugers Arch* **391**, 85–100.

Hermosura MC, Monteilh-Zoller MK, Scharenberg AM, Penner R & Fleig A (2002). Dissociation of the store-operated calcium current I_{CRAC} and the Mg-nucleotide-regulated metal ion current MagNuM. *J Physiol* **539**, 445–458.

Hoth M (1995). Calcium and barium permeation through calcium release-activated calcium (CRAC) channels. *Pflugers Arch* **430**, 315–322.

Hoth M & Penner R (1993). Calcium release-activated calcium current in rat mast cells. *J Physiol* **465**, 359–386.

Lee A, Scheuer T & Catterall WA (2000). Ca^{2+}/calmodulin-dependent facilitation and inactivation of P/Q-type Ca^{2+} channels. *J Neurosci* **20**, 6830–6838.

Lee A, Wong ST, Gallagher D, Li B, Storm DR, Scheuer T & Catterall WA (1999). Ca^{2+}/calmodulin binds to and modulates P/Q-type calcium channels. *Nature* **399**, 155–159.

Li WP, Tsiokas L, Sansom SC & Ma R (2003). Epidermal growth factor activates store-operated Ca^{2+} channels through an IP_3 independent pathway in human glomerular mesangial cells. *J Biol Chem* **279**, 4570–4577.

Parekh AB & Penner R (1997). Store depletion and calcium influx. *Physiol Rev* **77**, 901–930.

Peterson BZ, Demaria CD, Adelman JP & Yue DT (1999). Calmodulin is the Ca^{2+} sensor for Ca^{2+}-dependent inactivation of L-type calcium channels. *Neuron* **22**, 549–558.

Prakriya M & Lewis RS (2002). Separation and characterization of currents through store-operated CRAC channels and Mg^{2+}-inhibited cation (MIC) channels. *J General Physiol* **119**, 487–507.

Prakriya M & Lewis RS (2003). CRAC channels: activation, permeation, and the search for a molecular identity. *Cell Calcium* **33**, 311–321.

Rychkov G, Brereton HM, Harland ML & Barritt GJ (2001). Plasma membrane Ca^{2+} release-activated Ca^{2+} channels with a high selectivity for Ca^{2+} identified by patch-clamp recording in rat liver cells. *Hepatology* **33**, 938–947.

Sadeghi A, Doyle AD & Johnson BD (2002). Regulation of the cardiac L-type Ca^{2+} channel by the actin-binding proteins alpha-actinin and dystrophin. *Am J Physiol Cell Physiol* **282**, C1502–C1511.

Saimi Y & Kung C (2002). Calmodulin as an ion channel subunit. *Annu Rev Physiol* **64**, 289–311.

Spector I, Shochet NR, Blasberger D & Kashman Y (1989). Latrunculins – novel marine macrolides that disrupt microfilament organization and affect cell growth. I. Comparison with cytochalasin D. *Cell Motil Cytoskeleton* **13**, 127–144.

Trepakova ES, Gericke M, Hirakawa Y, Weisbrod RM, Cohen RA & Bolotina VM (2001). Properties of a native cation channel activated by Ca^{2+} store depletion in vascular smooth muscle cells. *J Biol Chem* **276**, 7782–7790.

Wu Z, Wong ST & Storms DR (1993). Modification of the calcium and calmodulin sensitivity of the type I adenylyl cyclase by mutagenesis of its calmodulin binding domain. *J Biol Chem* **268**, 23766–23768.

Xia XM, Fakler B, Rivard A, Wayman G, Johnson-Pais T, Keen JE, Ishii T, Hirschberg B, Bond CT, Lutsenko S, Maylie J & Adelman JP (1998). Mechanism of calcium gating in small-conductance calcium-activated potassium channels. *Nature* **395**, 503–507.

Yeromin AV, Roos J, Stauderman KA & Cahalan MD (2004). A store-operated calcium channel in *Drosophila* S2 cells. *J General Physiol* **123**, 167–182.

Zhang Z, Tang J, Tikunova S, Johnson JD, Chen Z, Qin N, Dietrich A, Stefani E, Birnbaumer L & Zhu MX (2001). Activation of Trp3 by inositol 1,4,5-trisphosphate receptors through displacement of inhibitory calmodulin from a common binding domain. *Proc Natl Acad Sci U S A* **98**, 3168–3173.

Zuhlke RD, Pitt GS, Deisseroth K, Tsien RW & Reuter H (1999). Calmodulin supports both inactivation and facilitation of L-type calcium channels. *Nature* **399**, 159–162.

Zuhlke RD & Reuter H (1998). Ca^{2+} sensitive inactivation of L-type Ca^{2+} channels depends on multiple cytoplasmic amino acid sequences of the alpha1C subunit. *Proc Natl Acad Sci U S A* **95**, 3287–3294.

Zweifach A & Lewis RS (1995). Rapid inactivation of depletion-activated calcium current (I_{CRAC}) due to local calcium feedback. *J General Physiol* **105**, 209–226.

Acknowledgements

We are grateful to Professor W. A. Catterall (University of Washington, USA) for providing us with the cDNA encoding CaM inhibitor peptide and Dr M. X. Zhu (Ohio State University, USA) for providing cDNA encoding the CaM mutant and wild type CaM. This work was supported by the Australian Research Council.